Magnetic structure and anisotropy of thin Fe films on Cu(001) substrates

R. Lorenz and J. Hafner
Institut für Theoretische Physik and Center for Computational Materials Science, Technische Universität Wien, Wiedner Hauptstraße 8-10, A-1040 Wien, Austria
(Received 22 April 1996)

We present a novel approach to the calculation of the spin structures and magnetic anisotropies in crystals and in thin films. Our technique is based on self-consistent real-space recursion calculations using a tight-binding-linear-muffin-tin-orbital (TB-LMTO) Hubbard Hamiltonian including spin-orbit coupling and allowing for arbitrary orientations of the local spin-quantization axes. It allows one to scan the magnetic energy continuously as a function of the direction of the magnetic moment and thus to avoid the computational problems that plague other techniques for the calculation of the magnetic anisotropy energies. The method also presents important advantages in determining the magnetic ground state in the presence of competing ferro- and antiferromagnetic interactions. Applications are presented for bulk iron, free-standing iron monolayers and for thin Fe overlayers on Cu(001) substrates. In the monolayer regime, we predict a perpendicular direction of the magnetic moment for free-standing fcc Fe(001) monolayers and for fcc monolayers on Cu(001) (with free surfaces and covered by Cu overlayers), with anisotropy energies of the order of 1–2 meV. We also present a detailed investigation of the spin structures and of the change from perpendicular to in-plane anisotropy with increasing thickness of the Fe films. We find that stable low-moment and metastable high-moment spin structures coexist in films with more than four monolayers. With increasing thickness of the films the perpendicular anisotropy decreases and for an ideal fcc geometry a transition to in-plane anisotropy can be expected around eight monolayers. [S0163-1829(96)00446-8]

I. INTRODUCTION

The magnetic properties of thin films are currently the object of intense research efforts. The motivation for this engagement is twofold: Ultrathin magnetic films epitaxially grown on nonmagnetic substrates are prototype systems for investigating magnetism in two dimensions, and the possibility to produce films and multilayers with perpendicular magnetic anisotropy for magnetooptic recording applications motivates an important technological interest (for recent reviews see, e.g., Allenspach,[1] Heinrich and Bland[2]). The topic of perpendicular magnetic anisotropy is a very challenging one, since the magnetostatic dipolar interactions always prefer in-plane orientation of the easy axis of magnetization. Since the pioneering experimental work of Gradmann[3,4] and the theoretical predictions of Gay and Richter[5] much effort has been spent investigating Fe, Co, and Ni films grown on noble-metals substrates. Among the heteroepitaxial systems that show strong perpendicular magnetic anisotropy (PMA) are Co/Au(111) thin films and superlattices,[6] Ni/Cu(001) (Refs. 7–9) and Ni/Cu(111) (Ref. 8) thin films, Co/Au(111) thin films and multilayers,[6,10] bcc Fe/Ag(001) (Refs. 11 and 12) and fcc Fe/Cu(001) (Refs. 13–21) thin films. In other epitaxial systems such as fcc Co/Cu(001) thin films,[22,23] fcc Co/Cu(111) superlattices,[10] and fcc Co/Au(111) superlattices[24] no evidence for a perpendicular anisotropy has been found.

In most systems perpendicular anisotropy is restricted to films with a few monolayers only. At a critical thickness the magnetization rotates into the plane of the film. It is generally accepted that the preference for a perpendicular orientation of the magnetic moment is due to the fact that for few monolayers the surface anisotropy can overcome the shape anisotropy, but it is not yet clear how the change in the sign of the uniaxial anisotropy is correlated with the crossover from two-dimensional XY to three-dimensional Heisenberg behavior as the film thickness increases.[8] Very recently a notable exception from this scenario has been detected in Ni/Cu(001) films where the crossover from in-plane to perpendicular anisotropy occurs with increasing film thickness.[7,9] It has been argued that this unusual thickness dependence follows from the intrinsic uniaxial anisotropy of the face-centered-tetragonal Ni lattice growing on the Cu substrate. This emphasizes the importance of even slight distortions of the pseudomorphic lattice of the film. Recent work has also drawn the attention to the importance of the morphology of the films, which depends in turn on the preparation conditions.

The situation proved to be particularly complex for fcc Fe/Cu(001) films. It has been shown that the magnetic properties depend very sensitively on the preparation conditions, but only slowly a consistent picture has emerged of how the differences in the preparation affect the growth, structure and morphology of the films. The recent experimental work has established a complex structural and magnetic phase diagram, with properties depending on the Fe film thickness t and other experimental parameters. The experiments studying the magnetic[13–21] and the structural[25–31] properties distinguish three different regions:

(i) Region I with $t \leqslant 5-6$ monolayers (ML) with a decreasing perpendicular anisotropy and a competition between a high-moment ferromagnetic[14–17] and low-moment antiferromagnetic[32,33] state. The structure of the film has mostly been described as tetragonally distorted ($c/a > 1$) fcc (Refs. 25, 28, and 20) or ''anisotropically distorted fcc.''[26] On the basis of recent high-precision LEED (low-energy electron diffraction) experiments, a complex (4×1) and

(5×1) reconstruction of films with 2 to 4 ML has been proposed.[30,31] The fcc (001) layers are flat only on average, the top layers show sinusoidal lateral shifts and vertical buckling. The interlayer distance is enhanced by about 5% between the top layer and the first subsurface layer, but otherwise bulklike. The surface reconstruction has been interpreted as representing a structural instability of the ferromagnetic fcc Fe phase. Insular growth has been observed for 1 and 2 ML. Layer-by-layer growth is achieved for thicker layers deposited at room temperature.[21,30,31] In films deposited at low temperature a surface roughness increasing with the thickness of the layer has been observed,[21] reflecting the kinetic limitations of low-temperature growth.

(ii) Films in region II (6–7 ML $\leqslant t \leqslant$ 10–12 ML) remain fcc with eventually a small tetragonal distortion and show paramagnetism or low-moment antiferromagnetism, depending on the temperature T_{prep} at which the films have been prepared. For films prepared at low temperature, the crossover from perpendicular to in-plane anisotropy occurs in the range of 5–6 ML.[15] Films prepared at room temperature show PMA in region II, the magnetization rotates into the plane of the film only after a thickness of 11–12 ML has been reached. The low-temperature prepared films in the transition range of 5–6 ML show a reversible spin-reorientation transition as a function of temperature: the direction of the magnetic moment changes from perpendicular to in plane and back as the temperature is increased and decreased.[14] The structure of the films has been described variously as isotropic fcc,[26,34] or as expanded[35] or compressed[28] face-centered tetragonal. The most recent high-precision LEED analysis[31] describes the structure as fcc, with a 5% expansion of the distance between the top- and the first-subsurface layer.

(iii) In region III with $t \geqslant$ 11–12 ML the films are bcc and ferromagnetic with in-plane anisotropy.

Hence there is evidence that the magnetic structure of thin Fe/Cu(001) films is influenced by many factors: (i) The competition between the ferromagnetic bcc structure and the antiferromagnetic fcc structure. The structural transition is believed to drive the magnetic transition observed at 11–12 ML. (ii) The possible tetragonal distortion of the fcc films. It has been shown that even small tetragonal distortions may affect the stability of the antiferromagnetic bulk fcc phase.[36] However, no comparable instability of the antiferromagnetic moments with respect to tetragonal distortions has been reported for thin films. (iii) The rather strong enhancement of the magnetism observed on the free surfaces of many magnetic systems and at the interfaces with nonmagnetic materials. The enhanced magnetic moment can influence the competition between ferro- and antiferromagnetic coupling. (iv) The competition between surface and shape anisotropy which is believed to be the driving mechanism of the reorientation transition observed at 5–6 ML. (v) The roughness of the films, at the free surface and at the interface between film and substrate.

In the present work we shall concentrate on those aspects that are directly related to the two-dimensional character of the magnetism in thin Fe/Cu(001) films by performing local-spin-density (LSD) calculations of the spin-polarized electronic structure, the magnetic ground state, and the magnetic anisotropy of films with up to 7 ML. We deliberately ignore for the moment all the aspects related to a distortion of the crystal structure in the films, a reconstruction of the surface, and to the roughness of surface or interface. Our aim is to establish the behavior of an ideally pseudomorphic film with flat surface and interface. There have been a few first-principles calculations of the magnetic structure of this complex system,[37–39] but so far no theoretical investigation of the magnetic anisotropy. The results of Fernando and Cooper[38] and of Fu and Freeman[37] show that in a free-standing Fe layer with the Cu lattice constant there is a ferromagnetic coupling between the surface (S) and the first subsurface (S-1) layer, but an antiferromagnetic coupling between the S-1 and S-2 layers. Kraft, Marcus, and Scheffler[39] have extended the analysis to a symmetric freestanding 11-layer slab and demonstrated that the antiferromagnetic coupling between neighboring layers continues from the S-1 layer to the center of the slab. All calculations agree in finding a strong enhancement of the magnetic moment at the surface, and, in contrast to the studies on bulk fcc and fct iron,[36] only a small variation of the magnetic moment with a tetragonal distortion of the structure of the films. No detailed investigation of the magnetic anisotropy of Fe/Cu(001) layers has been presented as yet.

One of the problems arising in films with competing ferro- and antiferromagnetic interactions is that the converged result is not necessarily independent of the initialization of the magnetic moments—it is conceivable that the self-consistent iterations converge to a metastable magnetic configuration because the flipping of a spin requires overcoming of a non-negligible energy barrier. In our study we use a real-space tight-binding linear-muffin-tin-orbital (TB-LMTO) technique that allows for arbitrary orientations of the local spin-quantization axes.[40–42] With this technique, the spins can continuously rotate from their initial directions into the equilibrium orientations. We find that this technique avoids running into metastable solutions. Moreover, it allows one to scan the magnetic energy continuously as a function of the direction of the moments and thus to calculate the magnetic anisotropy energy very accurately. In particular we find that by performing the calculations in real space we can avoid the serious problems with the convergence of the Brillouin-zone integrations that plague many of the techniques working in wave number space.

Our paper is organized as follows: In Sec. II we review very briefly our noncollinear spin-polarized TB-LMTO approach to magnetic anisotropy and discuss briefly benchmark applications to bulk iron. In Sec. III we discuss our results on freestanding and supported monolayers, Sec. IV is devoted to the investigation of magnetic anisotropy with varying film thickness.

II. THEORY

As pointed out by van Vleck,[43] the magnetic anisotropy originates from the spin-orbit coupling, hence it is a relativistic effect. In cubic crystals, due to the symmetry of the constant-energy surfaces, the leading contribution to the magnetic anisotropy energy (MAE) is of fourth order, hence MAE's are very small in crystals. As first pointed out by Néel,[44] due to the broken symmetry at the surface, lower-order perturbation contributions can contribute to the MAE.

Since the pioneering studies of Takayama, Bohnen, and Fulde[45] and of Gay and Richter,[5] two different approaches to the calculation of MAE's have been developed. The first approach uses perturbation theory within a semiempirical tight-binding framework, justified by the argument that the MAE is small compared to a characteristic bandwidth.[45–48] The published calculations rely on parametrized non-self-consistent TB Hamiltonians, this allows the analysis of trends, but makes quantitative predictions for selected systems quite difficult. The second approach relies on *ab initio* spin-polarized total-energy calculations, with spin-orbit coupling included either self-consistently within the scalar-relativistic approximation[49,50] or as a final perturbation to a calculation neglecting spin-orbit coupling[5,51–53] and using the force theorem.[54,55] The main difficulty with this approach arises from the fact that a change in the direction of the magnetic moment changes the occupation of the eigenstates only in a narrow region of the Brillouin zone, hence the $\vec{k}$-space integrations for the total energy are only very slowly convergent. To avoid the necessity to use a huge number of $\vec{k}$ points, Wang, Wu, and Freeman[53] introduced a *state-tracking* procedure, using information on the change of the band structure with increasing spin-orbit interaction to extrapolate the Brillouin-zone integrals.

A. Real-space tight-binding LMTO with local spin-quantization axes

Here we use an alternative approach based on a real-space tight-binding formulation of the scalar-relativistic Hamiltonian including spin-orbit coupling and magnetic dipolar interactions and allowing for arbitrary directions of the magnetic moments on each individual site. In the first step, we calculate self-consistently the direction and magnitude of the magnetic moments. This determines the magnetic structure, including the easy axis of magnetization. Compared to conventional spin-polarized band-structure calculations the fact that we allow for arbitrary (not necessarily collinear) directions of the spins makes it much easier to find the magnetic ground state. In particular the results are less dependent on the initialization of the magnetic moments, because their directions are allowed to change continuously (like in a Heisenberg magnet) whereas in a calculation with collinear moments (like in an Ising magnet) a spin flip always requires a finite energy. In the second step we can either apply a magnetic field perpendicular to the easy axis and calculate the MAE from the induced canting as a function of the applied field, or orient the moment perpendicular to the easy axis and follow its relaxation into the preferred direction under the influence of the magnetic torque forces, this yields directly the MAE as a function of the angle relative to the easy axis. Preliminary results on the MAE of iron monolayers obtained using this technique have been published recently.[42]

Our model Hamiltonian is given by

$$\mathbf{H}=\mathbf{H}_{\mathrm{band}}+\mathbf{H}_{\mathrm{exch}}+\mathbf{H}_{\mathrm{so}}+\mathbf{H}_{\mathrm{dip}},$$

where $\mathbf{H}_{\mathrm{band}}$ describes the nonmagnetic part of the band structure, $\mathbf{H}_{\mathrm{exch}}$ the magnetic exchange interactions, $\mathbf{H}_{\mathrm{so}}$ the spin-orbit coupling, and $\mathbf{H}_{\mathrm{dip}}$ the dipolar interactions between the magnetic moments leading to the shape anisotropy. The two-center tight-binding Hamiltonian $\mathbf{H}_{\mathrm{band}}$ and the exchange Hamiltonian $\mathbf{H}_{\mathrm{exch}}$ are derived from self-consistent scalar-relativistic spin-polarized band-structure calculations using the LMTO method[56,57] via a canonical transformation to the most localized TB basis.[58]

The formulation of the exchange part is based on the observation that the local exchange splitting Δ_{il} is exactly proportional to the local moment,

$$\Delta_{il}=I_l\mu_{il}$$

with an effective Stoner parameter I_l if the local exchange splitting is defined in terms of the difference in the position of the center of gravity of the spin-up and spin-down bands. Note that within the LMTO the center of gravity of the bands is given by the potential parameter C_{il}. Allowing in addition for a noncollinear orientation of the local spin-quantization axes $\vec{\zeta}_i$ we obtain a Hubbard-type exchange Hamiltonian

$$\mathbf{H}_{\mathrm{exch}}=-\frac{1}{2}\sum_{ilm}\Delta_{il}\sum_{ss'}X_{\zeta_i,ss'}c^{\dagger}_{ilms}c_{ilms'},$$

where

$$\mathbf{X}_{ss'}=\mathbf{D}_{\zeta_i}\sigma_z\mathbf{D}^{\dagger}_{\zeta_i}$$

is the local Pauli spin matrix σ_z referring to the local spin-quantization axis $\vec{\zeta}_i$ (the $\mathbf{D}_{\zeta_i}$ are the rotation matrices at site i, the c's are the electron creation and annihilation operators for electrons in a state with quantum numbers lms). That the effective Stoner parameter defined in terms of the center of gravity of the bands is a universal quantity for all transition metals and compounds has first been suggested by Himpsel[59] on the basis of photoemission and inverse photoemission investigations of the occupied and empty bands of a wide range of magnetic systems. Subsequently we have been able to show that the effective Stoner parameter I_l may be taken directly from the self-consistent LMTO calculations.[60–63] For d bands we find an almost universal value of $I_d=0.95\pm0.015$ eV/μ_B for all $3d$ metals and alloys, ranging from the ferromagnetic and antiferromagnetic crystalline metals over crystalline intermetallic compounds to the amorphous alloys with other transition metals (including $4d$ metals) and metalloids and to spin-glass systems. The result for the amorphous alloys and spin glasses is important because it demonstrates that the effective Stoner parameter is invariant even under large fluctuations of the local moments. Note that this value applies also to the ferrimagnetic moments carried by $4d$ metals in compounds and alloys that is induced by covalent interactions.[60,62] Self-consistent calculations for surfaces show that the universal proportionality between moment and exchange splitting holds with good accuracy also at the surface, eventually it is reduced by up to 5%. The universality of the effective Stoner parameter suggests that in the itinerant magnets the exchange interaction is essentially intra-atomic and has to be identified with Hund's rule exchange. This is also confirmed by the fact, already pointed out by Himpsel,[59] that the universal proportionality also applies to the magnetic moment and the splitting of the d levels in the free atom. For a more general discussion of the mapping of

the local-spin-density exchange Hamiltonian on Hubbard- (or Stoner-) type models, see, e.g., Anisimov, Zaanen, and Andersen.[64]

For the spin-orbit coupling we use a term given by

$$\mathbf{H}_{\mathrm{so}}=\sum_i \xi_i \vec{\sigma}_i \cdot \vec{L}_i ,$$

where ξ_i is the spin-orbit coupling matrix element calculated with the self-consistent scalar-relativistic wave functions.

The first step in our approach is the self-consistent calculation of the spin-polarized scalar relativistic band structure for the bulk crystal or for a slab model for the thin layer plus substrate within the LMTO technique in the atomic sphere approximation (ASA). The local spin-orbit coupling constant ξ_i is calculated in the final iteration.[56,51] For an LMTO with energy E, an energy-dependent spin-orbit coupling parameter $\xi_i(E)$ is defined by the expectation value of $\xi_i(\vec{r})$. In our calculations we used the spin-orbit coupling parameter calculated at the Fermi level. Coupling constants evaluated at the band centers are usually about 10% larger. We have verified that this difference does not affect the final results.

In the second step the self-consistent spin-dependent LMTO-ASA Hamiltonian is decomposed as defined above. The canonical transformation introduced by Andersen and Jepsen[58] leads to the two-center tight-binding Hamiltonian $\mathbf{H}_{\mathrm{band}}$ in the screened, most localized basis and in a Löwdin orthonormal representation. In the construction of the screened structure constants defining the TB-LMTO Hamiltonian, we consider an atomic environment up to the third neighbors. The calculations of the ground state are started with a random distribution of the spin-quantization axes and very small values ($\sim 0.05\mu_B$) of the local moments. For each site we calculate the local spin-polarized densities of state $n_{ilms}(E)^{\parallel,\perp}$ for spins parallel and perpendicular to the local quantization axis $\vec{\zeta}_i$. Integrating the $n_{ilms}(E)$ up to the Fermi level defines updated transverse and longitudinal components of the local magnetic moments relative to $\vec{\zeta}_i$, which gives a new direction for the quantization axis. This procedure is repeated until a self-consistent solution (no transverse moments relative to $\vec{\zeta}_i$) has been achieved. The advantage is that we essentially calculate the magnetic torque force that rotates the moments into the easy direction. For the calculation of the local densities of state (DOS) we use the real-space recursion technique of Haydock, Heine, and Kelly.[65] The recursion calculation is performed in a larger supercell, for bulk iron, for example, we use an ensemble of $8\times8\times8$ bcc elementary cells and periodic boundary conditions. In most cases nine recursion levels were used for the s orbitals, 12 for the p, and 27 for the d orbitals, together with a Beer-Pettifor terminator[66] to get a smooth density of states. We find that this gives sufficient resolution to grasp the small variations in the partial DOS of the in-plane and out-of-plane d orbitals with a changing direction of the magnetic moments that determine the magnetic anisotropy. To test the convergence of the MAE with respect to the number of recursion levels, their number has been increased up to 60 (using the extended supercell). Although such a high number is not necessary for achieving convergence of the total energies, it is advantageous for the discussion of the details of the spin-polarized DOS that determine the sign and magnitude of the MAE.

In the third step the magnetic anisotropy energy is calculated. This can be done in two different ways: (a) Adding a Zeeman term with a magnetic field perpendicular to the easy axis to the Hamiltonian and calculating self-consistently the induced rotation of the magnetic moments as a function of the applied field. (b) Orienting the magnetic moments perpendicular to the easy axis by applying a strong external field. Then the magnetic field is switched off and the moments are allowed to relax into the easy axis. During this relaxation the variation of the total energy with the direction of the moments is monitored continuously. In both cases the total energies are calculated self-consistently, including the double-counting corrections with the self-consistent charge and spin densities. The disadvantage of method (a) is that it yields the MAE only for discrete orientations of the moments and that one has to subtract the effect of the induced polarization. Approach (b) allows to scan the MAE continuously as a function of the direction of the magnetization. The difficulty is that after switching off the initial magnetic field the Hamiltonian is not completely self-consistent. Self-consistency is recovered only during the relaxation process. Both techniques lead to consistent results.

This is demonstrated in Fig. 1 at the example of fcc Fe monolayers on Cu(001) and Cu(111) substrates. With the ''scanning'' approach (b) the variation of the total energy shows small discontinuities at certain angles, arising from the changes in the band structure with the variation of the orientation of the magnetic moments. These are precisely the effects that make a $\vec{k}$-space calculation of the MAE so difficult. In our real-space approach the discontinuities are small and well controlled since we follow the changes in the band structure continuously as a function of the direction of the moments. This distinguishes our approach from the ''state-tracking'' procedure proposed by Freeman *et al.*:[52,53] they study the change in the band structure as a function of the strength of the spin-orbit coupling constant ξ at a few discrete orientations of the moments and determine the MAE by fitting these values by the expression appropriate to the given symmetry. In our case both the scanning and the discrete approach lead to a form of the MAE that follows very well the $E(\vartheta)=K_0+K_2\cos^2\vartheta$ law for uniaxial magnetic anisotropy. The calculations predict perpendicular anisotropy for Fe/Cu(001) and in-plane anisotropy for Fe/Cu(111), with MAE's of the order of 1 to 2 meV/atom. The detailed results for the iron monolayers on Cu will be discussed below in conjunction with the results for free monolayers.

Our approach is even sufficiently accurate for calculating the very small in-plane anisotropies in a monolayer with the easy axis in the plane of the layer. This can again be done via the ''scanning'' approach by orienting the magnetization along an off-symmetry direction in the plane and relaxing it into the easy direction, as shown in Fig. 2 for Fe/Cu(111). Due to the very small MAE, the scans become more noisy, but it is still perfectly possible to follow the angular dependence and to deduce the anisotropy constants. In this case we find an MAE of only 0.40 μeV/atom and an easy axis oriented along the basis vectors of the hexagonal surface cell.

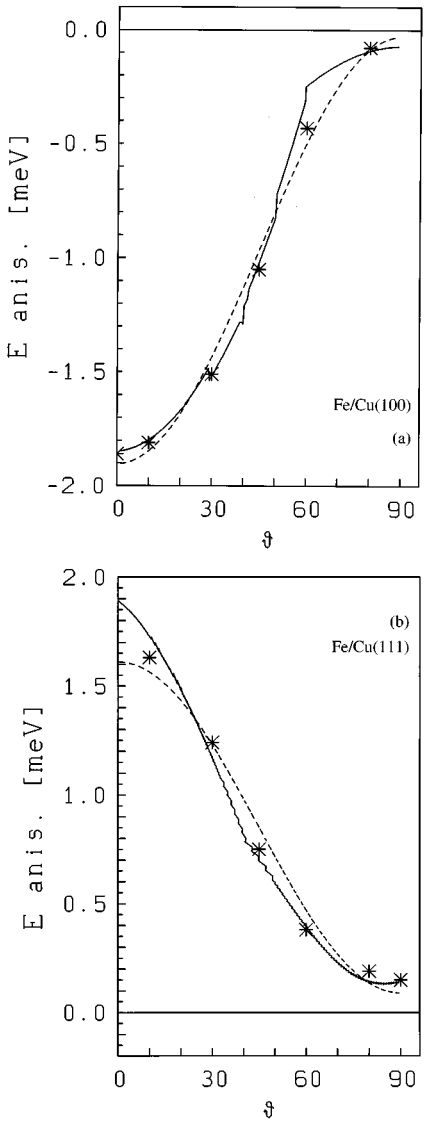

FIG. 1. Variation of the total magnetic energy as a function of the angle ϑ between the orientation of the magnetic moments and the surface normal for fcc Fe monolayers on Cu(001) (a) and Cu(111) (b). Full lines: results obtained via the ''scanning'' approach described in the text, stars: calculated for discrete orientations of the magnetic moments induced by applying a magnetic field perpendicular to the easy axis, broken lines: $\cos^2\vartheta$ fit.

B. The magnetic anisotropy of bulk iron: A test case

For bcc Fe at the experimental lattice constant we calculate a magnetic moment of $\mu = 2.24\mu_B$ with the easy axis in (001) direction. We obtain the magnetic anisotropy energy (MAE) as $\Delta E = E[001] - E[111] = -0.65$ μeV/atom. These values agree quite well with the calculations of Daalderop *et al.*[51] who found $\mu = 2.25\mu_B$ and $\Delta E = -0.4$ μeV/atom using a LMTO calculation with a set of about 500 000 $\vec{k}$ vectors. Early calculations of Fritsche *et al.*[67] predicted an MAE of $\Delta E = +7.4$ μeV/atom. The large difference has probably to be attributed to a too coarse mesh for the Brillouin-zone integrations. Compared to the experimental MAE [$\Delta E = -1.3$ μeV/atom (Ref. 68), $\Delta E = -1.4$ μeV/atom (Ref. 69)] even the more accurate values of the present work and of Daalderop *et al.* are still too small. Very recently, Trygg *et al.*[50] argued, following similar arguments of Jansen,[70] that orbital polarization corrections to local spin-density theory accounting in an approximate way for Hund's second rule are essential for achieving in many cases quantitative agreement of the calculated MAE with experiment. The polarization corrections also lead to an increase of the orbital moments, in the case of Fe from $0.05\mu_B$ to about $0.08\ \mu_B$.

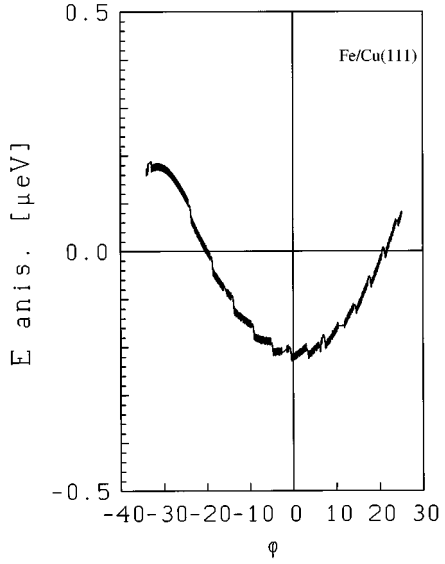

FIG. 2. Variation of the total magnetic energy of a fcc Fe monolayer on Cu(111) as a function of the angle ϕ of the direction of the magnetic moment relative to the basis vectors of the hexagonal surface cell. The calculation has been performed using the ''scanning'' approach.

III. MAGNETIC ANISOTROPY OF Fe MONOLAYERS

In this section we study the magnetic anisotropy of free-standing and supported Fe monolayers. For thin layers in general we used a cell with periodic boundary conditions in two dimensions only. The two-dimensional (2D) slabs consists of 25–32 layers (depending on the Fe-layer thickness t): three layers of empty spheres to account for the spilling out of charge into the vacuum, one to seven Fe layers, 3 Cu interface layers, and up to 19 Cu layers with the potential fixed at the Cu bulk values. In the case of Cu-covered iron ML on Cu(001) we used a similar geometry and for the free-standing iron layer we put three layers of empty spheres on both sides of the iron. Each (001) layer contains 288 atoms ([a $(12\sqrt{2}\times 12\sqrt{2})$ cell], each (111) layer 256 atoms [a (8×8) cell] (set up by repeating the $(\sqrt{2}\times\sqrt{2})$, respectively, (2×2) cell in the lateral directions).

A. Free-standing Fe monolayer

The LMTO calculations for the free-standing fcc Fe (001) layer with the in-plane lattice constant of Cu show a large moment of $\mu = 2.95\mu_B$ per Fe atom. This is caused by the missing neighbors on both sides of the layer. The enhanced moment is almost independent of the spin direction. From the TB-LMTO calculation we get an anisotropy energy of $\Delta E = -1.95$ meV per atom with the easy axis perpendicular

to the layer. If we decompose the MAE into its contributions from spin-orbit coupling and from the dipolar interactions, we find that the spin-orbit coupling prefers a PMA with $\Delta E_{so} = -2.17$ meV/atom, whereas the dipolar interactions prefer an in-plane orientation of the moments with $\Delta E_{dip} = 0.22$ meV/atom.

There have been a number of previous calculations of the MAE of free-standing Fe monolayers, based either on local-spin-density calculations, but using the force theorem for the MAE or on semiempirical tight-binding techniques. Using the first approach, Gay and Richter[5,71] found a pronounced increase of the moment compared to the bulk and a perpendicular anisotropy for fcc Fe(001) ML's whose magnitude depends on the assumed lattice constant ($\Delta E = -0.38$ meV/atom and $\mu = 3.2\mu_B$ for the lattice constant of Ag, $\Delta E = -0.61$ meV/atom and $\mu = 3.04\mu_B$ for the lattice constant of Cu). Li *et al.*[52] predicted a moment of $\mu = 3.13\mu_B$ with an in-plane orientation and an MAE of $\Delta E = +0.043$ meV/atom at the lattice constant of Ag. Using the state-tracking approach Wang *et al.*[53] investigated Fe-ML's with the Cu (Ag) lattice constants and predicted moments of $\mu = 3.04(3.22)\mu_B$ with perpendicular orientation and an MAE of $\Delta E = -0.42$ (0.37) meV/atom. The TB calculations are based on parametrized Hamiltonians, the results depend very sensitively on the details of this parametrization and on the filling of the *d* band. If the number of *d* electrons is assumed to be equal in the ML and in the free atom ($N_d = 8$ for Fe), Bruno[46] predicted essentially zero MAE for fcc Fe(001), and a small perpendicular MAE ($\Delta E = -0.61$ meV/atom) for Fe(111). Note that Bruno predicts a relatively large change of the orbital moment with a changing direction of the magnetic axis, in evident contrast to our results. Pick and Dreyssé[47] found in-plane anisotropies for both fcc Fe(001) and Fe(111) of 0.4 meV/atom and about 0.1 meV/atom, respectively. The authors result is presented in the form of a curve showing the variation of the MAE with the filling of the band at a fixed DOS (corresponding to a fixed potential), from this it is immediately clear that the result is very sensitive to the number of *d* electrons. In the TB calculations this is an input parameter, and not a result of a self-consistent calculation. The outcome is that both the perturbation techniques based on the use of the force theorem and the TB approaches must be considered as quite unreliable. The difference to the much larger perpendicular anisotropy found in our calculations is essential: for the thin films there is always a competition between the surface anisotropy that eventually favors perpendicular MA and the shape anisotropy coming from the dipolar interactions. Hence a perpendicular anisotropy can be sustained over a larger number of monolayers only if the surface anisotropy is large enough.

B. Fe monolayers supported on Cu substrates

In the next step we investigate the effect of the substrate. Since there is always a certain covalent coupling between the *d* bands of the overlayer and the substrate we expect that eventually the increase of the moment and hence the MAE is weaker than for the free ML. For the Fe/Cu(001) ML we calculate spin-orbit coupling parameters $\xi^{\uparrow}(E_F) = 59$ meV and $\xi^{\downarrow}(E_F) = 47$ meV for the spin-up and spin-down bands at the Fermi level. The coupling constants evaluated at the band centers are about 10% larger. These values are almost equal to the coupling constants calculated by Daalderop *et al.*[51] for bulk bcc Fe. The spin-orbit coupling constant for the Cu sites is larger, $\xi^{\uparrow,\downarrow}(E_F) = 108$ meV. For Fe/Cu(001) our calculations predict an easy axis oriented along the surface normal. The magnetic moment in the Fe monolayer is enhanced to $\mu = 2.7113\mu_B$ for perpendicular orientation, the moments changes only very little for in-plane orientation ($\mu = 2.7144\mu_B$). For comparison: Fu and Freeman,[37] Fernando and Cooper,[38] and Weinert and Blügel[72] predicted Fe moments of $\mu = 2.68\mu_B$, $\mu = 2.80\mu_B$, and $\mu = 2.85\mu_B$, respectively, and only a rather weak variation of the moment on relaxation of the adlayer distance to the substrate. The magnetic polarization of the Fe layer induces very small moments in the first vacuum layer ($\mu_{vac} = -0.02\mu_B$) and in the first and second Cu layers from the interface ($\mu_{Cu1} = 0.007\mu_B, \mu_{Cu2} = -0.012\mu_B$) via the covalent coupling to the Fe spin-up and spin-down bands. The anisotropy constant (equal to the MAE for in-plane to perpendicular orientation) is $\Delta E = E_{\perp} - E_{\parallel} = -1.87$ meV/atom, calculated via a fit of a $\cos^2\vartheta$ fit to the results obtained using both techniques (cf. Fig. 1 and Sec. II). These values are 3 orders of magnitude larger than the bulk MAE. Varying the spin-orbit coupling by $\pm 10\%$ changes the MAE only by $\pm 5\%$. This corresponds to the expected result: If we set $\mathbf{H} = \mathbf{H}_0 + \lambda \mathbf{H}_{so}$, the MAE should be proportional to $\lambda^2[\pm O(\lambda^4)]$ since the linear contribution is always zero due to time-reversal symmetry. The quadratic variation dominates for the monolayer and at the surface because of the broken symmetry.

For the Fe/Cu(111) monolayers, the spin-dependent difference in the spin-orbit coupling parameters is slightly larger: $\xi^{\uparrow} = 60$ meV, $\xi^{\downarrow} = 49$ meV. The enhancement of the magnetic moment in the Fe layer compared to the bulk value is smaller, $\mu = 2.561\mu_B$, almost independent of the direction of the moment. Again small moments are induced in the vacuum and Cu layers ($\mu_{vac} = -0.005\mu_B, \mu_{Cu1} = 0.010\mu_B, \mu_{Cu2} = -0.002\mu_B$). For this orientation of the substrate, our calculation predicts an in-plane orientation of the magnetic moment, with an MAE that is of the same order of magnitude as for the Cu(001) substrate, $\Delta E = E_{\perp} - E_{\parallel} = 1.52$ meV/atom. Decomposition into spin-orbit and dipolar contributions yields $\Delta E_{so} = 1.32$ meV/atom and $\Delta E_{dip} = 0.20$ meV/atom. Compared to the layers on (100) surfaces this means a small change in the dipolar interactions preferring in-plane anisotropy, but a change of sign in the PMA effects arising from the spin-orbit coupling.

As an additional step we calculated the magnetic properties of a Cu covered single Fe ML on Cu(001). Here we find a smaller value of the local magnetic moment of $\mu = 2.62\mu_B$ (compared to the free surface), but also the charge on the iron atoms are close to the bulk value. For the anisotropy we get $\Delta E = -1.41$ meV/atom with still out-of plane direction of the easy axis. Altogether we find that the MAE decreases from the free ML to the supported ML and the supported and covered ML, $\Delta E = -1.95$, -1.87, and -1.41 meV/atom, demonstrating that the surface anisotropy is larger than the interface anisotropy. Separating again the spin-orbit and dipolar contributions to the MAE we find (in the same sequence) $\Delta E_{so} = -2.17$, -2.04, and -1.56 meV/

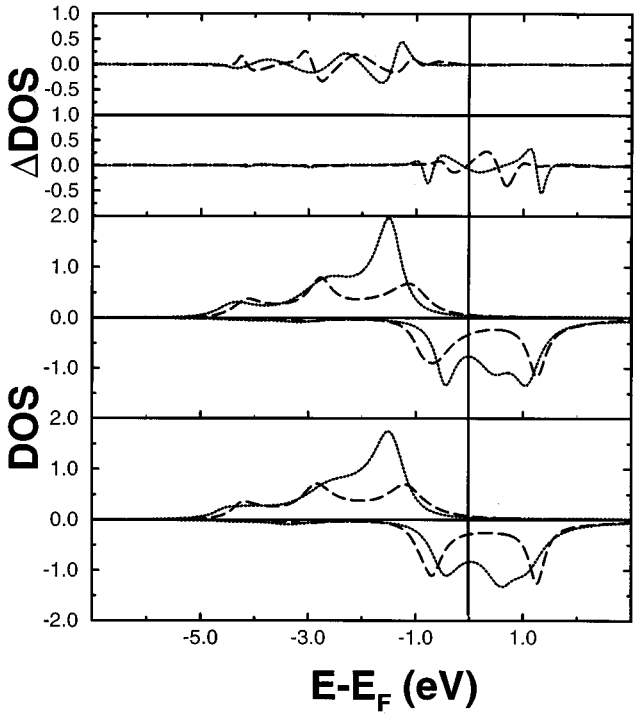

FIG. 3. Variation of the partial spin-polarized DOS of in-plane (dashed lines) and out-of-plane (dotted lines) *d* orbitals of Fe monolayers on Cu(100) substrates: Lower panel, magnetization oriented perpendicular to the surface (ground state); middle panel, magnetization parallel to the surface (stabilized by an external field); upper panels, differences in the partial spin-up and spin-down DOS's for in- and out-of-plane orientation of the moments, cf. text.

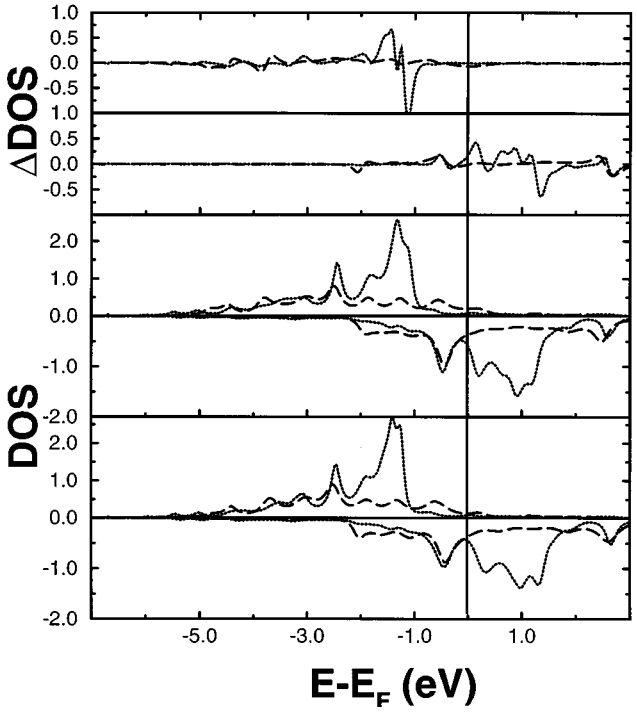

FIG. 4. Same as Fig. 3, but for Fe/Cu(111) monolayers where the easy axis lies in the surface-plane.

atom, and $\Delta E_{\mathrm{dip}} = 0.22$, 0.17, and 0.15 meV/atom. This shows that the decreasing strength of the PMA is caused by decreasing spin-orbit effects.

The contribution of the spin-orbit coupling to the MAE has often been attributed, at least in part, to a change of the orbital moment on a reorientation of the magnetic axis.[46] Here we have found that these changes are very small. Hence the origin of the MAE must be associated with changes in the band structure arising from the broken crystalline symmetry in the presence of a global axis of magnetization. The physical effects determining the MAE becomes clear if we consider the change of the occupation of the out-of-plane orbitals [$d_{3z^2-r^2}$, d_{xz}, and d_{yz} for the (001) surface] and the in-plane ($d_{x^2-y^2}$, d_{xy}) orbitals with the re-orientation of the direction of magnetization [see Fig. 3, Fig. 4 reports the same information for the Fe/Cu(111) monolayer]. The calculations have been performed for a large supercell containing more than 8000 atoms, and using sixty recursion level to achieve a good energy resolution for the *d* band.

We discuss first the case of Fe/Cu(100). One of the first points to note is that in the ML the majority *d* band is always completely filled, in contrast to bulk Fe. This is a consequence of the band-narrowing resulting from the reduction of the Fe-Fe coordination number at the surface or interface and leads automatically to an enhancement of the magnetic moment. Hence in some sense, a ML of Fe can be considered as a strong ferromagnet. We shall find that this is important in determining the exchange interactions close to the surface. The partial in- and out-of-plane DOS's of the spin-up electrons change only little with a reorientation of the magnetization (except for a slight sharpening of the main peak in the out-of-plane DOS). Integrated up to the Fermi level the effect of the changes in the spin-up bands on the magnetic total energy compensate completely. More distinct changes are found in the spin-down bands. The occupied part of the spin-down bands shows a single dominant peak at a binding energy of 0.4 eV for the out-of-plane, and at 0.65 eV for the in-plane orbitals. This peak is always sharper for the orbitals extending in the direction of the magnetic moment. For the in-plane orbitals this yields a certain redistribution of the occupation of the states within 1 eV from the Fermi level without a pronounced effect on the MAE, but for the out-of-plane orbitals it means that states that are immediately at E_F for the in-plane orientation of the magnetic moment are shifted to binding energies of about 0.2–0.3 eV.

The situation is similar for Fe/Cu(111) monolayers (see Fig. 4). Again we find that the changes in the occupancy of the in- and/or out-of-plane orbitals compensate when integrated over the occupied part of the spin-up band. The spin-down band is significantly broader for the (111) than for the (100) films, and there are small changes in the orbital occupancies on a forced reorientation of the magnetic moment pointing into the opposite direction. Both the band contribution ΔE_{so} and the dipolar contribution lead to an in-plane anisotropy.

IV. THIN Fe FILMS ON Cu(001) SUBSTRATES

A. Stable and metastable magnetic configurations

For thicker films problems appear already at an even more elementary level. For bulk fcc Fe the antiferromagnetic type I (AuCuI-type order) state has a lower energy than the ferromagnetic state, but it is well known that the magnetic

TABLE I. Average magnetic moment $\overline{\mu}$ per Fe atom, layer-resolved magnetic moments μ_i (in Bohr magnetons μ_B), difference in total energy ΔE_{tot} (in eV), change of the average magnetic moment on reorientation of the axis of magnetization $\Delta\overline{\mu}$ (decomposed into its spin and orbital contributions, in μ_B), and anisotropy energy ΔE (decomposed into spin-orbit and dipolar contributions ΔE_{so} and ΔE_{dip} (in meV) for fcc Fe films of t monolayers on Cu(001).

LMTO calculations									
t	1	2	3	4	5 [a]	5 [b]	6	7 [a]	7 [b]
$\overline{\mu}$	2.72	2.70	2.65	1.40	1.59	0.56	0.87	1.11	0.46
μ_1	2.72	2.86	2.87	2.86	2.92	2.79	2.81	2.85	2.79
μ_2		2.53	2.50	2.40	2.49	2.24	2.28	2.43	2.24
μ_3			2.58	-2.01	2.42	-1.68	-2.38	2.11	-1.89
μ_4				2.35	-2.24	1.69	-2.35	-2.19	1.61
μ_5					2.35	-2.26	2.32	-2.18	-1.42
μ_6							2.54	2.22	2.07
μ_7								2.54	-2.19
ΔE_{tot}					-0.049			-0.103	

TB-LMTO-Hubbard calculations							
t	1	2	3	4	5	6	7
$\overline{\mu}$	2.71	2.49	2.45	1.41	0.58	0.82	0.46
μ_1	2.71	2.76	2.82	2.81	2.75	2.77	2.77
μ_2		2.22	2.34	2.38	2.27	2.20	2.25
μ_3			2.19	-1.95	-1.70	-2.36	-1.90
μ_4				2.41	1.86	-2.31	1.63
μ_5					-2.27	2.11	-1.45
μ_6						2.51	2.15
μ_7							-2.21
$\Delta\overline{\mu}$	0.012	0.020	0.016	0.009	0.010	0.127	0.014
$\Delta\overline{\mu}_{spin}$	0.010	0.018	0.014	0.010	0.016	0.090	0.011
$\Delta\overline{\mu}_{orb}$	0.002	0.002	0.002	-0.001	-0.006	0.037	0.003
ΔE	-1.87	-1.30	-1.15	-1.00	-0.65	-1.18	-0.33
ΔE_{so}	-2.04	-1.70	-2.71	-1.56	-1.25	-2.10	-1.03
ΔE_{dip}	0.17	0.40	0.56	0.56	0.60	0.92	0.70

[a]Metastable state.
[b]Ground state.

ground state is a noncollinear state in the form of a spin spiral.[73–75] Previous slab-calculations for free-standing Fe-layers[37–39] indicate that layer-type antiferromagnetic coupling can exist in the subsurface layers. The problem with standard spin-polarized band-structure calculations is that the local magnetic moments have to be initialized at nonzero values to break the symmetry of the paramagnetic state. This initialization creates a bias in a certain direction, and it is not sure that the calculation converges to the true ground state because a spin flip always costs a finite energy. The problem is less severe when we allow for a continuous rotation of the magnetic moments. Indeed we find that in some cases this allows us to show that the solution of the standard LMTO represents only a metastable magnetic state.

The results of the standard LMTO calculations are compiled in the top of Table I. All calculations are initialized with local moments of $\mu_i = 0.05\mu_B$. For up to three monolayers the films are entirely ferromagnetic, with an enhanced moment at the surface. For $t=4$, the second subsurface $(S\text{-}2)$ layer couples antiferromagnetically, for $t=5$ $(S\text{-}3)$, and for $t=6$ $(S\text{-}2)$ and $(S\text{-}3)$ show negative polarization [i.e., the coupling is antiferromagnetic between $(S\text{-}1)$ and $(S\text{-}2)$, and between $(S\text{-}3)$ and $(S\text{-}4)$]. Our results agree with those of Kraft *et al.*[39] in that the first two top layers couple ferromagnetically, whereas the interior of the film shows antiferromagnetic coupling. However, there are differences in the details. These are not unexpected, since their results refer the symmetric, unsupported films. For $t=5$ the three top layers couple ferromagnetically and only the moments in the fourth layer are oriented in the antiparallel direction. For $t=6$ the magnetic configuration is $\uparrow\uparrow\downarrow\downarrow\uparrow\uparrow$, i.e., we find an antiferromagnetic coupling between bilayers. This type of coupling persists for $t=7$, with the only difference that the three top layers couple ferromagnetically. Note that this implies that the average magnetic moment is larger for $t=7$ than for $t=6$.

The LMTO calculations do not necessarily find the magnetic ground state. This appears from the comparison with the noncollinear TB-LMTO calculations (see the bottom of Table I). The LMTO and TB-LMTO calculations agree for $t=1-4$, but for $t=5$ the TB-LMTO predicts negative polarization for $(S\text{-}2)$ and $(S\text{-}4)$ (i.e., a spin-configuration $\uparrow\uparrow\downarrow\uparrow\downarrow$ against $\uparrow\uparrow\uparrow\downarrow\uparrow$ and a lower average magnetization. Repeating the LMTO calculations with the moments initial-

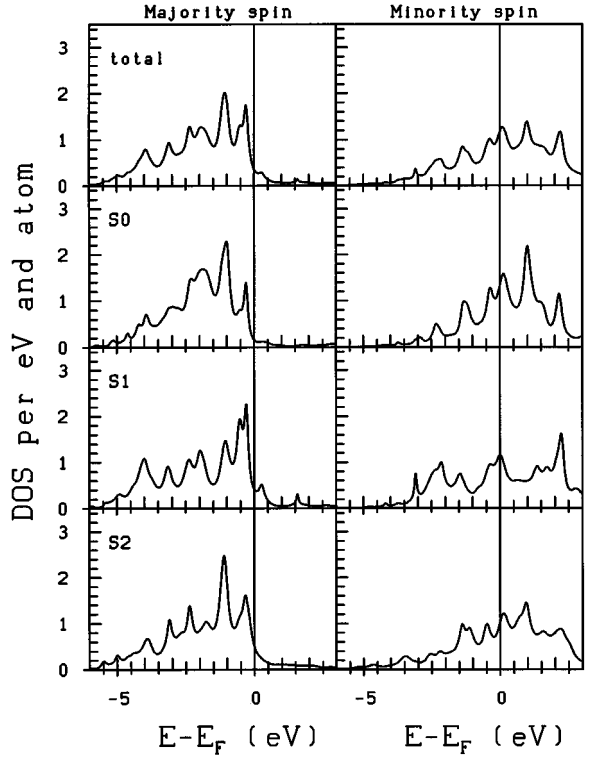

FIG. 5. Total and layer-resolved spin-polarized d-electron density of states for a three-layer film of fcc Fe on Cu(100). Left column, DOS for majority spins; right column, DOS for minority spins. All three layers couple ferromagnetically.

ized at small values pointing in the right directions shows the new configuration to be the ground state, whereas the other configuration turns out to be a metamagnetic state. Note that the stable solution shows relatively low moments in the interior of the film, in contrast to the metastable solution where all layers have moments larger than the bulk value. For $t=6$ we find again a good agreement between both types of calculations and a high-moment solution. The calculations for $t=7$ also show a metamagnetic high-moment solution for the $\vec{k}$-space collinear calculation, and a layered antiferromagnetic state ($\uparrow\uparrow\downarrow\uparrow\downarrow\uparrow\downarrow$) with low moments in the interior of the film. For the ground-state configurations the average magnetic moment in the film decreases first monotonically up to $t=5$, but increases again for $t=6$ and decreases further for $t=7$.

The total and layer-resolved densities of states for the three-layer film (Fig. 5) show the effects that stabilize ferromagnetic order in the limit of very thin films: at the free surface and at the Fe/Cu interface the reduced number of Fe-Fe neighbors leads to a narrowing of the Fe d band, in particular antibonding spin-up (majority) states close to the Fermi level are shifted to higher binding energies. The consequence is that the spin-up bands in the surface layer and in the interface layer are fully occupied, leading to the enhanced magnetic moment. The effect is weaker at the Fe/Cu interface than at the free surface because the Fe-Cu interaction tends to broaden the bands. As we have already mentioned this means that we have strong magnetism in the boundary layers. In the interior of the film the band narrowing is of course reduced and the spin-up band overlaps with

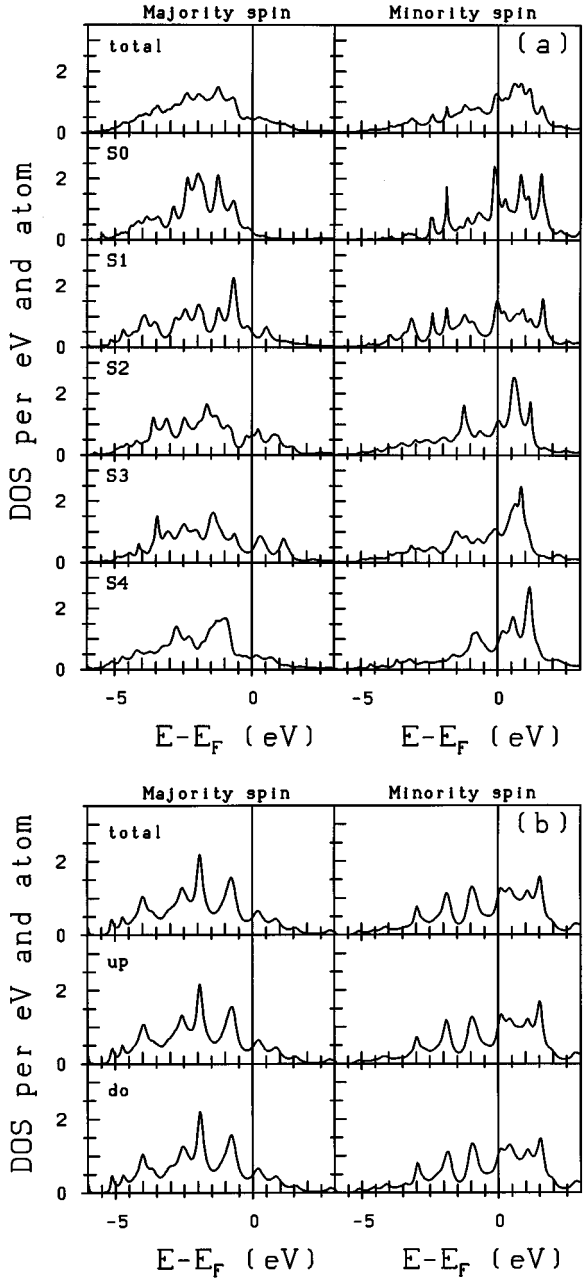

FIG. 6. (a) Total and layer-resolved spin-polarized d-electron density of states for five-layer films of fcc Fe on Cu(100). Left column, DOS for majority spins; right column, DOS for minority spins (relative to the local spin orientation in each layer). The spin configuration is $\uparrow\uparrow\downarrow\uparrow\downarrow$, starting from the free surface. (b) shows for comparison the spin-polarized DOS in bulk fcc Fe with layered antiferromagnetism. Panels labeled ''up'' refer to layers with the spin pointing in the positive direction, ''do'' to layers with antiferromagnetic polarization, cf. text.

the Fermi edge and we have weak magnetism. Note the pronounced differences in the DOS of the minority band.

In the thicker layers [see Fig. 6(a) for $t=5$] the DOS of the surface layer retains the same character, but that of the inner layer is already quite close to that in bulk fcc Fe with layered antiferromagnetism [shown for comparison in Fig. 6(b)]. Note that we show in the left column the majority-spin DOS in each layer, and in the right column the minority-spin

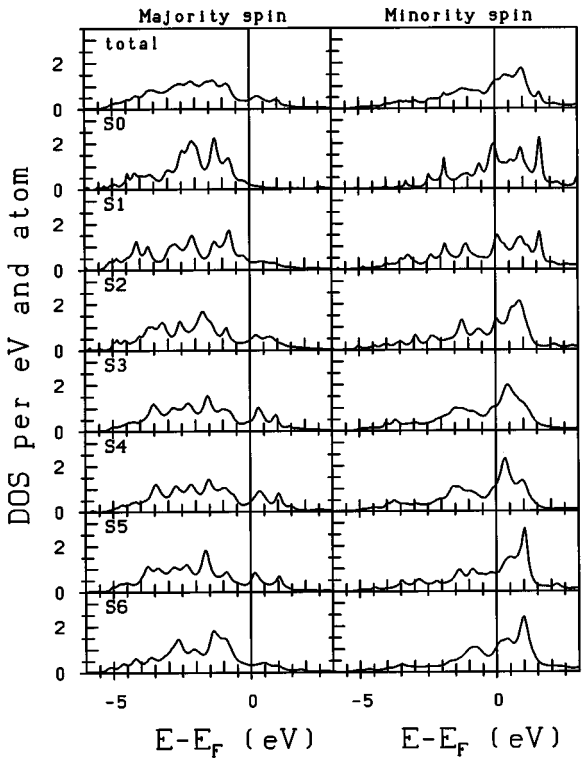

FIG. 7. Total and layer-resolved spin-polarized d-electron density of states for a seven-layer film of fcc Fe on Cu(100). Left column, DOS for majority spins; right column, DOS for minority spins (relative to the local spin orientation in each layer). The spin configuration is $\uparrow\uparrow\downarrow\uparrow\downarrow\uparrow\downarrow$, starting from the free surface, cf. text.

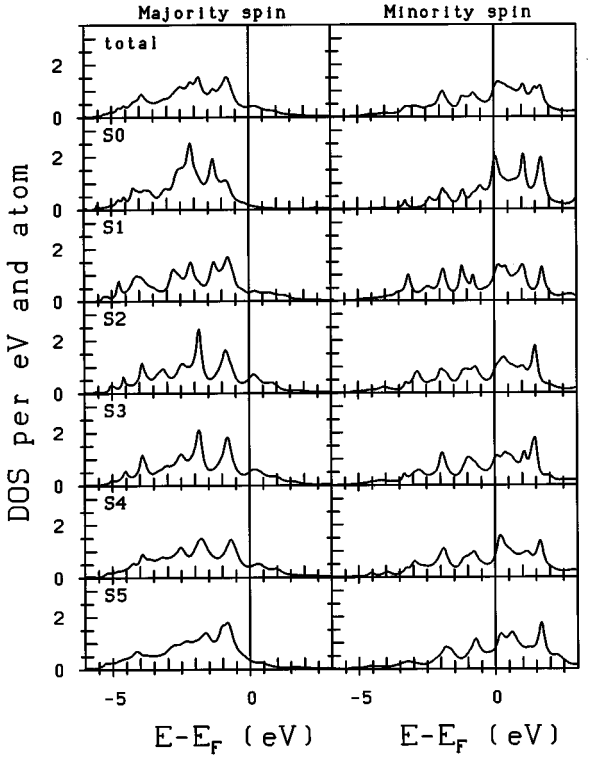

FIG. 8. Total and layer-resolved spin-polarized d-electron density of states for a six-layer film of fcc Fe on Cu(100). Left column, DOS for majority spins; right column, DOS for minority spins (relative to the local spin orientation in each layer). The spin configuration is $\uparrow\uparrow\downarrow\downarrow\uparrow\uparrow$, starting from the free surface, cf. text.

DOS, for a layer with both ferro- and antiferromagnetic components in the spin-polarization this makes more sense than a classification in terms of spin-up and spin-down electrons. In the regions with layer-type antiferromagnetic coupling, the DOS is characteristically different from that in the ferromagnetic regions: in both the majority and minority bands we observe a pronounced DOS minimum at E_F and a characteristic two-peak structure just above E_F. This structure is an immediate consequence of the layer-type interactions. The picture is even further away from rigidly shifted spin-up and spin-down bands than in the ferromagnetic case. An important point to note is that the formation of a DOS minimum at the Fermi edge stabilizing the AFM structure depends on a relatively large bandwidth and a substantial overlap of the band with the Fermi level. The surface-induced band narrowing is hence responsible for the existence of a ferromagnetic surface bilayer. At the Fe/Cu interface the DOS is of an intermediate character, but the AFM coupling to the neighboring layer is just marginally stable. The same conclusions can be drawn from the discussion of the layer-resolved DOS's of the seven-layer film (see Fig. 7).

The existence of an AFM bilayer coupling in a six-layer film is a peculiar case (see Fig. 8). The layer-resolved DOS shows a relatively small variation across the film, with a character that is intermediate between the AFM and FM DOS in the other films. The approximate inversion symmetry of the film seems to be important in stabilizing this solution.

B. Variation of the magnetic anisotropy with the film thickness

The anisotropy energy ΔE (the results given in Table I refer to the entire film) decreases nonmonotonically with increasing thickness of the Fe film. From $t=1$ to $t=4$ we first observe a steady decrease reducing the MAE to about half the value it has in a supported monolayer. For $t=5$ the strong decrease of the average magnetic moment due to the appearance of a second layer with antiparallel magnetization is accompanied by a corresponding decrease in the MAE. For $t=6$ the AFM bilayer coupling and the increased average moment result in a MAE that is nearly as large than in a three-layer film. For $t=7$ the magnetic structure of the film returns to a layered AFM, and correspondingly to a low MAE.

The overall decrease of the MAE is dominated by an increasing positive dipolar contribution and a slowly decreasing and fluctuating spin-orbit term. While the increasing importance of the dipolar interactions is easy to understand, the variations in the spin-orbit energies are related in a complex way to the variation of magnetic moments and of the d bands on a reorientation of the global magnetic moment. As for the monolayers, we find that in all films the change in the spin and in the orbital moments with a reorientation of the magnetic axis is rather small. Hence the MAE is determined by band effects. In Figs. 9–12 we analyze again the spin-polarized layer-resolved DOS $n_{i,d}(E)$ projected on the in-plane and out-of-plane d orbitals and their variation

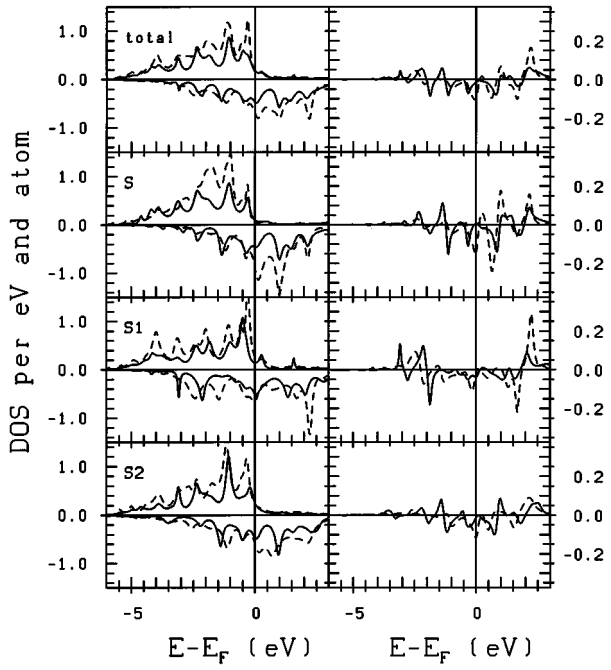

FIG. 9. Total and layer-resolved spin-polarized electronic DOS of a three-layer Fe film on Cu(100), projected on in-plane (full lines) and out-of-plane (broken lines) Fe *d* orbitals. The left column shows the DOS's for the ground state (magnetic moments perpendicular to the surface), the right column the difference in the minority-spin DOS's for perpendicular and in-plane orientation of the moments, cf. text.

$\Delta n_{i,d}(E)$ with the direction of the magnetization. The left column shows the projected DOS's for the ground state (i.e., with the moment perpendicular to the film), the right column the change of the DOS's of the minority spins if the moment is forced into an in-plane orientation (as for the monolayers we find that the effect of the changes in the majority-spin DOS compensate after integration over all occupied states). For the FM three-layer film we find a situation similar to that in the Fe/Cu(100) monolayer: the changes induced in the DOS of the in-plane orbitals largely compensate after taking the integral up to the Fermi level. The dominant effect on the MAE is the shift of states from immediately at E_F for in-plane magnetization to higher binding energies. This effect manifests itself in Fig. 9 by a sharp minimum in $\Delta n_{i,d}(E)$ for the out-of-plane orbitals. The effect is present in all three layers, but it is larger on the surface than at the interface and in the interior of the film.

For the five-layer film with two FM layers at the surface and three AFM layers below, this effect appears only in the FM-coupled surface and first-subsurface layer, but not in the AFM layers deeper in the film (see Fig. 10). For the six-layer film with the AFM bilayer coupling, strong contributions to the MAE come from the two top layers, weaker contributions from the two layers at the Fe/Cu interface (see Fig. 11). For the seven-layer film we are back at the situation already found for five layers: in the interior of the film, the reorientation of the magnetic axis leaves the partial projected DOS's almost unaffected, contributions to the MAE come only from the two top layers (see Fig. 12).

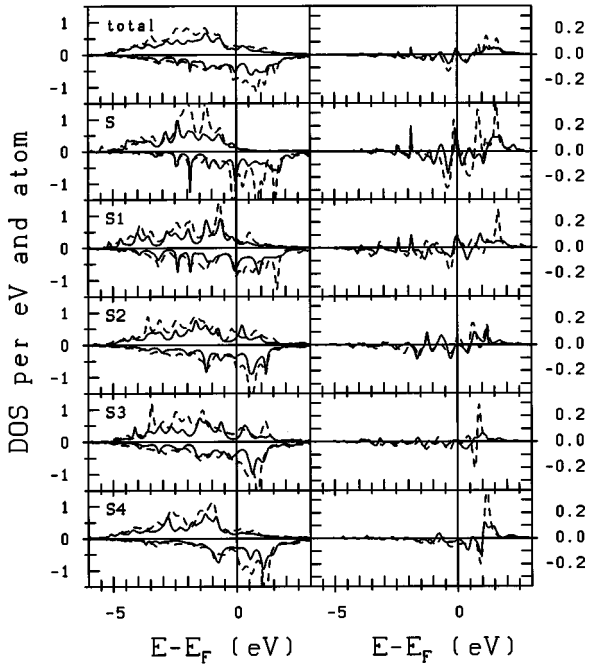

FIG. 10. Same as Fig. 9, but for a five-layer Fe/Cu(100) film.

V. DISCUSSION AND SUMMARY

We have presented calculations of the magnetic structure and of the uniaxial and planar anisotropies of thin films of Fe on Cu(100) substrates. Our approach exploits essentially the magnetic-torque force restoring the magnetic moment to the easy axis. By following continuously the changes introduced in the electronic structure as a function of the direction of the magnetization, it avoids the cumbersome computational

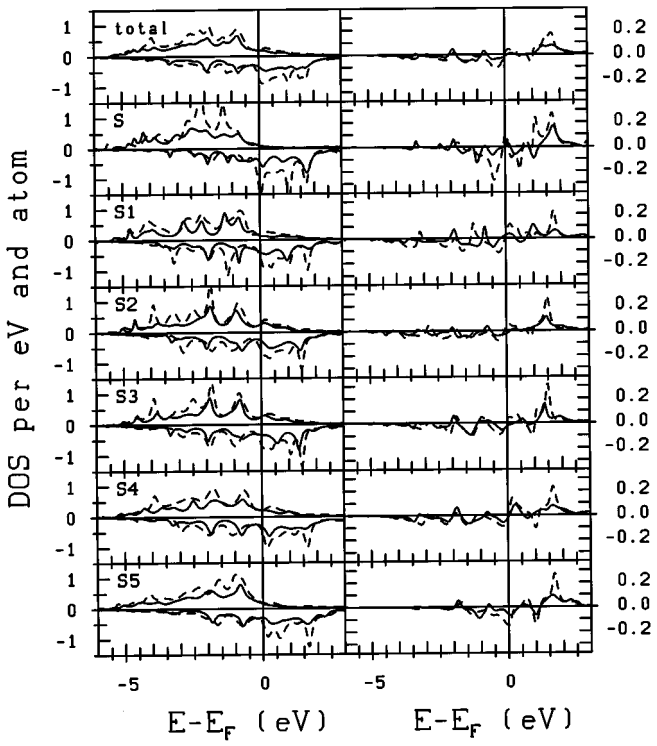

FIG. 11. Same as Fig. 9, but for a six-layer Fe/Cu(100) film.

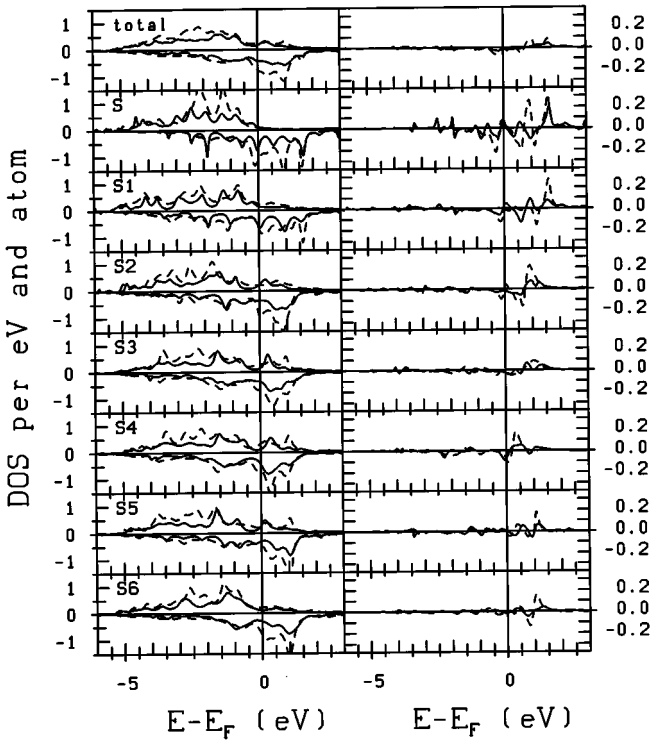

FIG. 12. Same as Fig. 9, but for a seven-layer Fe/Cu(100) film.

problems that plague other techniques based on total-energy calculations. We have shown that for the extremely small magnetic anisotropy energy in bulk iron, our technique leads to good agreement with the computationally much more demanding $\vec{k}$-space techniques. We have also demonstrated that the technique is sufficiently accurate for calculating the planar anisotropy in monolayers that is 3 orders of magnitude lower than the uniaxial thin-film and surface anisotropies. The detailed investigation of Fe monolayers has led to a clear picture of the relative importance of the surface and interface anisotropies, and of the effect of nonmagnetic coverages of the magnetic film: replacing a free surface by an interface always leads to a reduction of the MAE because the hybridization of the *d* states across the interface limits the increase of the magnetic moment to smaller values than those characteristic for the free surface.

We have studied in detail the magnetic structure and anisotropy of thin Fe films on Cu(100) as a function of the film thickness. Ideal pseudomorphic growth of fcc films has been assumed. Up to three monolayers the magnetic film is ferromagnetic, for thicker films ferromagnetic coupling is restricted to the two topmost layers, whereas antiferromagnetic coupling dominates in the deeper layers. In films with five or more monolayers metamagnetic high- and low-moment states have been identified. The coexistence of different locally stable magnetic configurations is clearly a consequence of the competition between ferro- and antiferromagnetic exchange interactions. We have also shown that the magnetic ground state can correspond to layer-type antiferromagnetism in the deeper layers of the film (like in the five- and seven-layer films), or to an antiferromagnetic coupling between bilayers with parallel magnetic moments (like in the six-layer film).

The simultaneous occurrence of high- and low-moment solutions might explain some of the conflicting experimental results presented in the literature. We anticipate that in films with steps or with a certain roughness of the surface and/or interface frustration of the exchange interactions will lead to complex noncollinear spin structures with canted spins near the steps.

We have calculated the magnetic anisotropy as a function of the film thickness. The results show a slow decrease of the PMA as a consequence of the shifting balance between the spin-orbit effects preferring PMA and the dipolar interactions leading to an in-plane ground state. In addition we find a pronounced dependence of the MAE on the magnetic ground state of the film: low-moment states also show lower anisotropy, bilayer coupling tends to enhance the anisotropy.

ACKNOWLEDGMENTS

This work has been supported by the Austrian Ministry for Science and Research within the Materials Research Program (Project ''Magnetism on the Nanometer Scale,'' No. GZ 45.378/2-IV/6/94).

[1] R. Allenspach, J. Magn. Magn. Mater. **129**, 160 (1994).
[2] *Ultrathin Magnetic Structures I, II*, edited by B. Heinrich and J. A. C. Bland (Springer, Berlin, 1994).
[3] U. Gradmann, Ann. Phys. **7**, 91 (1966).
[4] U. Gradmann, J. Magn. Magn. Mater. **54**, 733 (1986).
[5] J. G. Gay and R. Richter, Phys. Rev. Lett. **56**, 2728 (1986).
[6] R. Allenspach, M. Stampanoni, and A. Bischoff, Phys. Rev. Lett. **65**, 3344 (1990).
[7] B. Schulz and K. Baberschke, Phys. Rev. B **50**, 13467 (1994).
[8] F. Huang, M. T. Kief, G. J. Mankey, and R. F. Willis, Phys. Rev. B **49**, 3962 (1994).
[9] G. Bochi, C. A. Ballentine, H. E. Inglefield, C. V. Thomson, R. C. O'Handley, Hans J. Hug, B. Stiefel, A. Moser, and H. J. Güntherodt, Phys. Rev. B **52**, 7311 (1995).
[10] C. H. Lee, H. Hee, F. J. Lamelas, W. Vavra, C. Uher, and R. Clarke, Phys. Rev. B **42**, 1066 (1990).
[11] B. Heinrich, K. B. Urquardt, A. S. Arrott, J. F. Cochran, K. Martle, and S. T. Purcell, Phys. Rev. Lett. **59**, 1756 (1987).
[12] Z. Q. Qiu, J. Pearson, and S. D. Bader, Phys. Rev. Lett. **70**, 1006 (1993).
[13] C. Liu, E. R. Moog, and S. D. Bader, Phys. Rev. Lett. **60**, 2422 (1988).
[14] D. P. Pappas, K. P. Kämper, and H. Hopster, Phys. Rev. Lett. **64**, 3179 (1990).
[15] R. Allenspach and A. Bischof, Phys. Rev. Lett. **69**, 3385 (1992).
[16] J. Thomassen, F. May, B. Feldmann, M. Wuttig, and H. Ibach, Phys. Rev. Lett. **69**, 3831 (1992).
[17] Dongqi Li, M. Freitag, J. Pearson, Z. Q. Qiu, and S. D. Bader, Phys. Rev. Lett. **72**, 3112 (1994).
[18] F. Scheurer, R. Allenspach, P. Xhonneux, and E. Courtens, Phys. Rev. B **48**, 9890 (1993).
[19] D. J. Keavney, D. F. Storm, J. W. Freeland, I. L. Grigorov, and J.

C. Walker, Phys. Rev. Lett. **74**, 4531 (1995).
[20] R. D. Ellerbeck, A. Fuest, A. Schatz, W. Keune, and R. A. Brand, Phys. Rev. Lett. **74**, 3053 (1995).
[21] J. Giergiel, J. Shen, J. Woltersdorf, A. Kirilyuk, and J. Kirschner, Phys. Rev. B **52**, 8528 (1995).
[22] D. Pescia, G. Zampieri, M. Stampanoni, G. L. Bona, R. F. Willis, and F. Meier, Phys. Rev. Lett. **58**, 933 (1987).
[23] P. Krams, F. Lauks, R. L. Stamps, B. Hillebrands, and G. Güntherodt, Phys. Rev. Lett. **69**, 3674 (1992).
[24] T. Kingetsu and K. Sakai, Phys. Rev. B **48**, 4140 (1993).
[25] A. Clarke, P. J. Rous, M. Arnott, G. Jennings, and R. F. Willis, Surf. Sci. **292**, L843 (1987).
[26] H. Magnan, D. D. Chandresis, B. Villette, O. Heckmann, and J. Lecante, Phys. Rev. Lett. **67**, 859 (1991).
[27] D. D. Chambliss, K. E. Johnson, R. J. Wilson, and S. Chiang, J. Magn. Magn. Mater. **121**, 1 (1993).
[28] M. Wuttig and J. Thomassen, Surf. Sci. **282**, 237 (1993).
[29] M. Wuttig, B. Feldmann, J. Thomassen, F. May, H. Zillgen, A. Brodde, H. Hannemann, and H. Neddermeyer, Surf. Sci. **291**, 14 (1993).
[30] S. Müller, P. Bayer, A. Kinne, and K. Heinz, Surf. Sci. **322**, 21 (1995).
[31] S. Müller, P. Bayer, C. Reischl, K. Heinz, B. Feldmann, H. Zillgen, and M. Wuttig, Phys. Rev. Lett. **74**, 765 (1995).
[32] W. A. A. Macedo and W. Keune, Phys. Rev. Lett. **61**, 475 (1988).
[33] W. A. A. Macedo, W. Keune, and R. D. Ellerbrock, J. Magn. Magn. Mater. **94**, 552 (1991).
[34] P. Bayer, S. Müller, P. Schmailzl, and K. Heinz, Phys. Rev. B **48**, 17611 (1993).
[35] A. Clarke, P. J. Rous, M. Arnott, G. Jennings, and R. F. Willis, Surf. Sci. **192**, L843 (1987).
[36] S. S. Peng and H. J. F. Jansen, J. Appl. Phys. **69**, 6132 (1991).
[37] C. L. Fu and A. J. Freeman, Phys. Rev. B **35**, 925 (1987).
[38] G. W. Fernando and B. R. Cooper, Phys. Rev. B **38**, 3016 (1988).
[39] T. Kraft, P. M. Marcus, and M. Scheffler, Phys. Rev. B **49**, 11511 (1994).
[40] R. Lorenz and J. Hafner, J. Magn. Magn. Mater. **139**, 209 (1995).
[41] R. Lorenz and J. Hafner, Phys. Rev. Lett. **74**, 3688 (1995).
[42] R. Lorenz and J. Hafner, J. Phys.: Condens. Matter **7**, L253 (1995).
[43] J. H. van Vleck, Phys. Rev. **52**, 1178 (1937).
[44] L. Néel, J. Phys. Rad. **15**, 505 (1954).
[45] H. Takayama, K. P. Bohnen, and P. Fulde, Phys. Rev. B **14**, 2287 (1976).
[46] P. Bruno, Phys. Rev. B **39**, 865 (1989).
[47] Š. Pick and Dreyssée, Phys. Rev. B **48**, 13588 (1993).
[48] M. Cinal, D. M. Edwards, and J. Mathon, Phys. Rev. B **50**, 3754 (1994).
[49] R. H. Victora and J. M. McLaren, Phys. Rev. B **47**, 11 583 (1993).
[50] J. Trygg, B. Johanson, O. Erikson, and J. M. Wills, Phys. Rev. Lett. **75**, 2871 (1995).
[51] G. H. O. Daalderop, P. J. Kelly, and M. F. H. Schuurmans, Phys. Rev. B **41**, 11 919 (1990); **42**, 7270 (1990).
[52] C. Li, A. J. Freeman, H. J. F. Jansen, and C. L. Fu, Phys. Rev. B **42**, 5433 (1990).
[53] D. S. Wang, R. Wu, and A. J. Freeman, Phys. Rev. Lett. **70**, 869 (1993).
[54] A. R. Mackintosh and O. K. Andersen, in *Electrons at the Fermi Surface*, edited by M. Sprinford (Cambridge University Press, Cambridge, England, 1980), Chap. 53.
[55] V. Heine, in *Solid State Physics—Advances in Research and Applications*, edited by H. Ehrenreich, D. Turnbull, and F. Seitz (Academic Press, New York, 1980), Vol. 35, p. 114.
[56] O. K. Andersen, Phys. Rev. B **12**, 3060 (1975).
[57] H. L. Skriver, *The LMTO Method* (Springer, Berlin, 1984).
[58] O. K. Andersen and O. Jepsen, Phys. Rev. Lett. **53**, 2571 (1984).
[59] F. J. Himpsel, Phys. Rev. Lett. **67**, 2363 (1991).
[60] I. Turek, Ch. Becker, and J. Hafner, J. Phys.: Condens. Matter **4**, 7257 (1992).
[61] J. Hafner, M. Tegze, and Ch. Becker, Phys. Rev. B **49**, 285 (1994).
[62] Ch. Becker and J. Hafner, Phys. Rev. B **50**, 3933 (1994).
[63] Ch. Becker, J. Hafner, and R. Lorenz, J. Magn. Magn. Mater. **151-158**, 619 (1996).
[64] V. I. Anisimov, J. Zaanen, and O. K. Andersen, Phys. Rev. B **44**, 943 (1991).
[65] R. Haydock, V. Heine, and M. J. Kelly, J. Phys. C **8**, 2591 (1975).
[66] N. Beer and D. Pettifor, in *The Electronic Structure of Complex Systems*, edited by P. Phariseau and W. M. Temmerman (Plenum, New York, 1984).
[67] L. Fritsche, J. Noffke, and H. Eckhardt, J. Phys. F **17**, 943 (1987).
[68] P. Escudier, Ann. Phys. (N.Y.) **9**, 125 (1975).
[69] M. B. Stearns, in *3d, 4d, and 5d Elements, Alloys and Compounds*, edited by H. P. J. Wijn, Landolt-Börnstein, New Series, Group 3, Vol. 19a (Springer, Berlin, 1986).
[70] H. J. F. Jansen, J. Appl. Phys. **67**, 4555 (1990).
[71] R. Richter and J. G. Gay, *Growth, Characterization and Properties of Ultrathin Magnetic Films and Multilayers*, edited by B. T. Janker, J. P. Heremans, and E. E. Marinero, MRS Symposia Proceedings No. 151 (Materials Research Society, Pittsburgh, 1989), p. 3.
[72] M. Weinert and S. Blügel, in *Magnetic Multilayers*, edited by L. H. Bennett and R. E. Watson (World Scientific, Singapore, 1993).
[73] V. Heine, A. I. Liechtenstein, and O. N. Mryasov, Europhys. Lett. **12**, 545 (1990); M. U. Lucchini and V. Heine, *ibid.* **14**, 609 (1991).
[74] O. N. Mryasov, A. I. Liechtenstein, L. M. Sandratskii, and V. A. Gubanov, J. Phys.: Condens. Matter **3**, 7683 (1991).
[75] O. N. Mryasov, V. A. Gubanov, and A. I. Liechtenstein, Phys. Rev. B **45**, 12 330 (1992).